Available online at www.sciencedirect.com
ScienceDirect
Catalysis Today 133–135 (2008) 231–238
CATALYSIS TODAY
www.elsevier.com/locate/cattod

Dry reforming of methane over nickel catalysts supported on the cuspidine-like phase $Nd_4Ga_2O_9$

Verónica García [a,b], Maria Teresa Caldes [b,*], Olivier Joubert [b], German Sierra Gallego [c], Catherine Batiot-Dupeyrat [c], Yves Piffard [b], Jorge Andrés Moreno [a]

[a] *Univesidad de Antioquia, Institute of Chemistry, A.A. 1226, Medellin, Colombia*
[b] *Institut des Matériaux Jean Rouxel, UMR CNRS 6502, 2 rue de la Houssinière, BP 32229, 44322 Nantes Cedex 03, France*
[c] *Laboratoire de Catalyse en Chimie Organique, UMR CNRS 6503, ESIP, Université de Poitiers, 40 Avenue du recteur Pineau, 86022 Poitiers, France*

Available online 1 February 2008

Abstract

Carbon dioxide reforming of methane was studied over Ni catalysts supported on the cuspidine-like phase $Nd_4Ga_2O_9$. Attempts to prepare two types of materials were undertaken by combustion synthesis: $Nd_4Ga_{2(1-x)}Ni_{2x}O_{9-x}$ compounds and $Ni/Nd_4Ga_2O_9$ samples containing 5, 10 and 15 wt% of Ni. The Ni-substituted $Nd_4Ga_2O_9$ phases could not be obtained, whereas the $Ni/Nd_4Ga_2O_9$ catalysts were prepared successfully. All catalysts exhibit activity towards dry reforming of methane. The best catalytic activity was observed at 800 °C for the catalyst with a Ni content of 10% reduced at 700 °C. After 12 h on steam, Ni particles were 10–20 nm in size, and no carbonaceous deposits were observed. A strong and complex interaction between nickel and the cuspidine $Nd_4Ga_2O_9$ support exists. This feature coupled with the moderate basicity of the cuspidine-type support could explain the weak Ni coarsening observed under reaction conditions and the good resistance to coking of the catalysts.

Keywords: Dry reforming; Syngas; Cuspidine-type phases; Ni catalysts

1. Introduction

Recently, special attention has been paid to hydrogen production because of its use as clean energy source in fuel cells. Hydrogen is mainly produced by reforming hydrocarbons and significant efforts have been devoted to the development of hydrocarbons reforming systems. Obviously, the process would be simpler if fuel cells could run on hydrocarbon fuels directly.

Solid oxide fuel cells (SOFCs) generate energy power by diffusion of O^{2-} anions (obtained by reduction of O_2 at the cathode of the cell) through an electronically insulating membrane (electrolyte) and subsequent combination with protons or protonic species. In principle, any fuel that combines with oxygen can be used to generate electricity. Also, since SOFCs operate at temperatures for which catalytic-combustion rates are significant (~600–1000 °C), direct oxidation of the fuel is possible at the anode, provided that this anode is able to catalyze the reaction between fuel and oxygen anions and to transport electrons toward the outer circuit. In addition, since other reforming reactions occur simultaneously at the anode (fuel + CO_2, fuel + H_2O and CO + H_2O) the anode in a fuel cell running on hydrocarbons, should also exhibit a good catalytic activity for dry and steam reforming.

Usually, in SOFCs, the anode is a ceramic–metallic (cermet) composite. In most cases the ceramic compound is the same as that used as electrolyte and Ni plays the role of electron conductor. A major problem with direct oxidation of hydrocarbons on a Ni–cermet anode is that Ni catalyses the cracking reaction yielding carbonaceous species on the anode. Therefore, an anode for direct oxidation of hydrocarbon fuels in SOFCs must simultaneously resist to coke accumulation, conduct electrons and exhibit a good catalytic activity towards hydrocarbon reforming reactions taking place in the fuel cell.

Recently, Joubert et al. [1,2] have reported a new family of anionic (O^{2-}) conductors based on the cuspidine phase $Nd_4Ga_2O_9$, with possible use as electrolyte and/or as Ni–cermet anode in SOFCs. Since the fuel most frequently used is natural gas, mainly composed of methane, the aim of this work

* Corresponding author.
E-mail address: maite.caldes@cnrs-imn.fr (M.T. Caldes).

0920-5861/$ – see front matter © 2007 Elsevier B.V. All rights reserved.
doi:10.1016/j.cattod.2007.12.061

is to evaluate the catalytic activity of several $Nd_4Ga_2O_9$ supported Ni catalysts for dry reforming of methane.

2. Experimental

$Nd_4Ga_{2(1-x)}Ni_{2x}O_{9-x}$ compounds and the $Ni/Nd_4Ga_2O_9$ catalysts containing 5, 10 and 15 wt% of Ni, were prepared by combustion synthesis [3]. EDTA ($C_{10}H_{16}N_2O_8$) was selected as the fuel and complexing agent. Metal nitrates were used as metal precursors and as oxidizing agents (NO_3^- groups).

A stoichiometric combustion reaction implies that the oxygen content of oxidant is equal to that necessary to oxidize the organic fuel completely. The method of Jain et al. [4] can be used to calculate the oxidizing/reducing character of the mixture. The global reaction between metal nitrates and EDTA to form Ni^{2+}-substituted cuspidine compounds can be written as follows:

$$32Nd(NO_3)_3 + 16(1-x)Ga(NO_3)_3 + 16xNi(NO_3)_2 + 2(9-x)C_{10}H_{16}N_2O_8 \rightarrow 8Nd_4Ga_{2(1-x)}Ni_{2x}O_{9-x} + 20(9-x)CO_2 + 10(9-x)N_2 + 16(9-x)H_2O$$

The stoichiometric ratio between nitrates and EDTA corresponds to eight NO_3^- groups per molecule of EDTA. Since fuel-deficient and stoichiometric combustion reactions are usually highly exothermic and difficult to control [5], a fuel-rich composition (20 wt% excess of EDTA) was used to prepare the samples.

For the synthesis of $Nd_4Ga_{2(1-x)}Ni_{2x}O_{9-x}$ series, separate aqueous solutions of metal nitrates were prepared from $Nd(NO_3)_3{\cdot}6H_2O$, $Ga(NO_3)_3{\cdot}9H_2O$ and $Ni(NO_3)_2{\cdot}6H_2O$. These solutions were titrated by thermogravimetric analysis. The EDTA solution was prepared by dissolving the required quantity in a minimum volume of dilute aqueous ammonia. Solutions of metal nitrates and EDTA were mixed together in the required molar ratio yielding transparent metal nitrate–EDTA solutions which were dehydrated at ~100 °C on a hot plate, leading to a highly viscous gel. In fact, the versatile ability of EDTA as a complexing agent for a variety of metal ions avoids selective precipitation. As soon as the gel was formed, the temperature of the hot plate was increased to ~300 °C. At this stage, the gel swelled and auto-ignited in a controlled and self-sustaining manner to produce voluminous blackish powder precursor that was ground and heated at 900 °C for 6 h.

For $Ni/Nd_4Ga_2O_9$ catalysts, neodymium and gallium nitrate solutions were mixed in the required molar ratio to form $Nd_4Ga_2O_9$ and the appropriate amount of nickel nitrate solution was added along with the required volume of EDTA solution to obtain a fuel-rich combustion reaction (20 wt% of excess of EDTA). Next steps of the synthesis are the same as those described previously for $Nd_4Ga_{2(1-x)}Ni_{2x}O_{9-x}$ compounds.

Powder X-ray diffraction (XRD) patterns of the final products were recorded using an INEL position-sensitive detector (Cu Kα1: λ = 1.540598 Å). Structure refinements were carried out using the program FULLPROF [6].

BET surface area was measured on a Micromeritics ASAP 2010 M apparatus, employing N_2. Prior to measurements, the samples were degassed at 100 °C for 5 h in high vacuum.

Transmission electron microscopy (TEM) was carried out on a field emission gun microscope Hitachi HF2000 operating at 200 kV, equipped with an energy dispersive X-ray (EDX) analyzer. The compounds were gently ground in ethanol and microcrystals were deposited on a holed carbon film supported by a copper grid.

The temperature-programmed reduction (TPR) studies were performed in a chemisorption unit Micromeritics AutoChem 2910 with samples of ~50 mg. Before reaction, the samples were treated with helium at 500 °C for 10 min and cooled to room temperature. The TPR experiments were carried out under a 5.1% H_2/Ar mixture flowed at 50 mL min^{-1} through the sample, raising the temperature at 10 °C min^{-1} up to 950 °C. The consumption of hydrogen was monitored on-line with a thermal conductivity detector.

The reforming reaction was carried out in a continuous-flow quartz fixed-bed under atmospheric pressure, by passing a flow of methane (10%), carbon dioxide (10%) and helium (80%) as carrier gas, over ~50 mg of catalyst at 700 and 800 °C, the total flow rate being equal to 100 mL min^{-1} and the space velocity 1.2×10^5 mL g^{-1} h^{-1}. The temperature was increased at 10 °C min^{-1} from room temperature to 800 °C and maintained for several hours. The catalyst was reduced under pure hydrogen (10 mL min^{-1}) for 1 h at 700 or 850 °C prior to each catalytic reaction run. The composition of the reactants/products mixture was analysed with an on-line mass spectrometer. All the catalytic experiments were performed twice.

3. Results and discussion

3.1. Catalyst characterization

The XRD patterns of the $Nd_4Ga_{2(1-x)}Ni_{2x}O_{9-x}$ materials, obtained upon heating at 900 °C for 6 h the precursor resulting from the combustion reaction, are shown in Fig. 1. For the compounds with $x = 0$, 0.0125 and 0.025, respectively, a pure

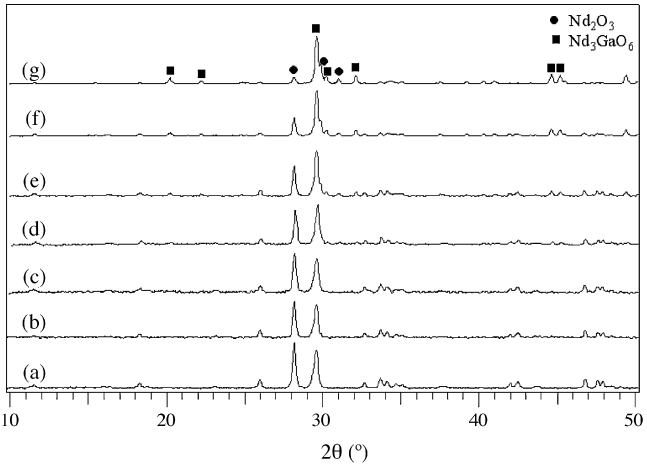

Fig. 1. XRD patterns of the $Nd_4Ga_{2(1-x)}Ni_{2x}O_{9-x}$ materials: (a) $x = 0$, (b) $x = 0.0125$, (c) $x = 0.025$, (d) $x = 0.05$, (e) $x = 0.1$, (f) $x = 0.15$ and (g) $x = 0.2$.

$Nd_4Ga_2O_9$ phase and pure Ni-substituted $Nd_4Ga_2O_9$ phases seem to be obtained. On the other hand, for the compounds with $x = 0.05$, 0.1 and 0.15 though $Nd_4Ga_2O_9$-type patterns are clearly identified, the XRD reveal the presence of several impurities: Nd_3GaO_6 and Nd_2O_3. For $x = 0.2$ the majority phase is $Nd_3Ga_2O_6$.

In order to confirm the replacement of Ga^{3+} by Ni^{2+} in the cuspidine structure, a Rietveld analysis of the XRD data was undertaken for the compounds with $x = 0$, 0.0125 and 0.025. The refinement was carried out in space group $P2_1/c$ by using the $Nd_4Ga_2O_9$ structure as starting model.

The cuspidine structure can be described as built up from ribbons of edge sharing NdO_6 octahedra running parallel to the c axis, and pairs of GaO_4 tetrahedra forming Ga_2O_7 groups (Fig. 2). Such ribbons are interconnected by corner sharing to create an ''octahedral'' framework to which Ga_2O_7 groups are linked via vertices. The aliovalent substitution of Ga^{3+} by Ni^{2+} implies the formation of charge-compensating oxygen vacancies. Since a threefold coordination is unlikely for Ga^{3+}, oxygen vacancies are only possible on sites which are bonded to Nd^{3+} only.

As can be seen in Fig. 3 for $x = 0.025$ as representative example, quite satisfactory refinements were achieved. However, the cell parameters calculated for $x = 0.0125$ and 0.025 are nearly identical (within three times the estimated standard deviations (E.S.D.s)) to those refined for $x = 0$ (see Table 1).

Such results strongly suggest that the replacement of Ga^{3+} by Ni^{2+} in the cuspidine structure does not occur, probably because neodymium atoms do not accept the fivefold coordination. If Ni-substituted $Nd_4Ga_2O_9$ phases could not be obtained, extra peaks corresponding to Nd_2O_3 and NiO should be observed; however as this attempt corresponds to a very small substitution ratio, we are dealing with trace amounts of impurity phases, which therefore can hardly be detected.

The XRD patterns corresponding to $Nd_4Ga_2O_9$ supported Ni catalysts are shown in Fig. 4. The diffraction peaks of Ni/$Nd_4Ga_2O_9$ catalysts coincide with those of the $Nd_4Ga_2O_9$ phase. No extra peaks of Ni-containing species were detected for the 5% Ni/$Nd_4Ga_2O_9$ catalyst. The first noticeable NiO peaks appear in the 10% Ni/$Nd_4Ga_2O_9$ XRD pattern. However, they are rather broad and this could well be a consequence of a very small crystallite size. For the 15% Ni/$Nd_4Ga_2O_9$ catalyst, the XRD pattern reveals the presence of trace amounts of the Nd_2NiO_4 phase.

The surface area of the 5% and 10% Ni/$Nd_4Ga_2O_9$ catalysts are 3.2 m^2/g and 5.7 m^2/g, respectively.

Fig. 5 displays the normalized TPR profiles of the Ni/$Nd_4Ga_2O_9$ catalysts as well as that of a pure $Nd_4Ga_2O_9$ sample.

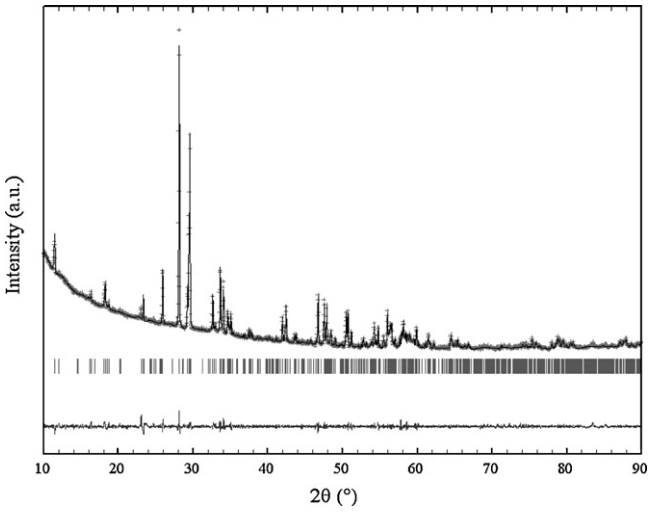

Fig. 3. Observed, calculated, Bragg reflections and difference profile for $Nd_4Ga_{0.95}Ni_{0.05}O_{9.975}$. Reliability factors: $R_{wp} = 12.6$, $R_B = 4.56$ and $\chi^2 = 3.43$.

Table 1
Cell parameters of $Nd_4Ga_{2(1-x)}Ni_{2x}O_{9-x}$ compounds as a function of x

x	a (Å)	b (Å)	c (Å)	β (°)
0	7.7677 (4)	10.9750 (4)	11.4786 (4)	109.047 (3)
0.0125	7.7689 (2)	10.9750 (3)	11.4772 (4)	109.054 (2)
0.025	7.7686 (3)	10.9731 (4)	11.4771 (5)	109.060 (2)

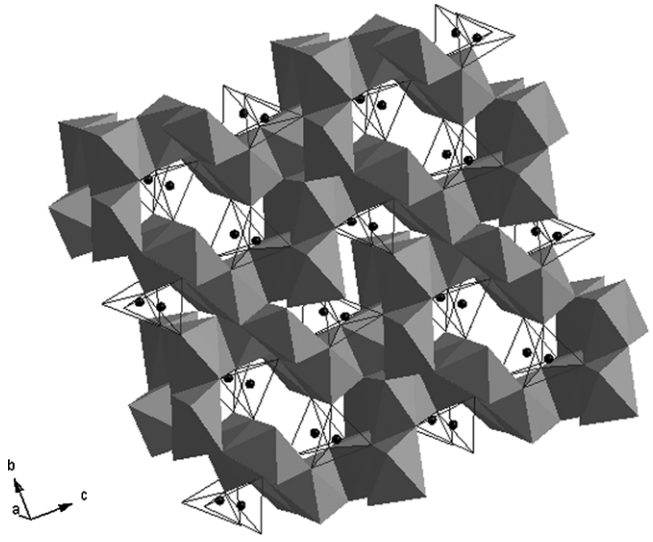

Fig. 2. [1 0 0] View of the cuspidine structure $Nd_4Ga_2O_9$ showing ribbons of edge sharing NdO_6 octahedra and Ga_2O_7 groups (open faces polyhedra).

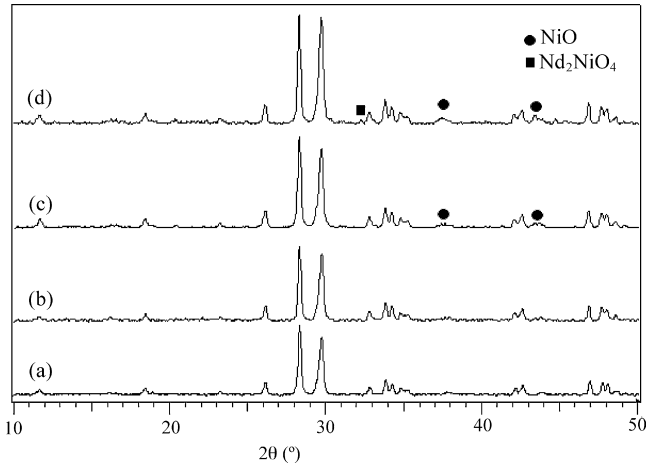

Fig. 4. XRD patterns of (a) $Nd_4Ga_2O_9$; (b) 5% Ni/$Nd_4Ga_2O_9$; (c) 10% Ni/$Nd_4Ga_2O_9$ and (d) 15% Ni/$Nd_4Ga_2O_9$.

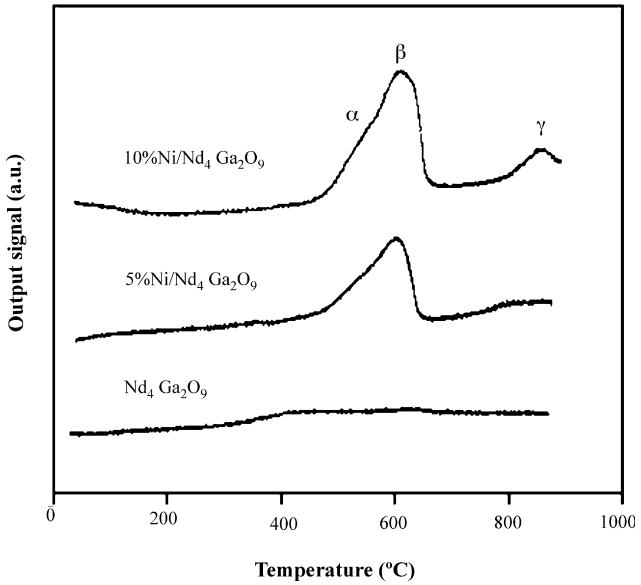

Fig. 5. TPR profiles of $Nd_4Ga_2O_9$ and Ni/$Nd_4Ga_2O_9$ catalysts.

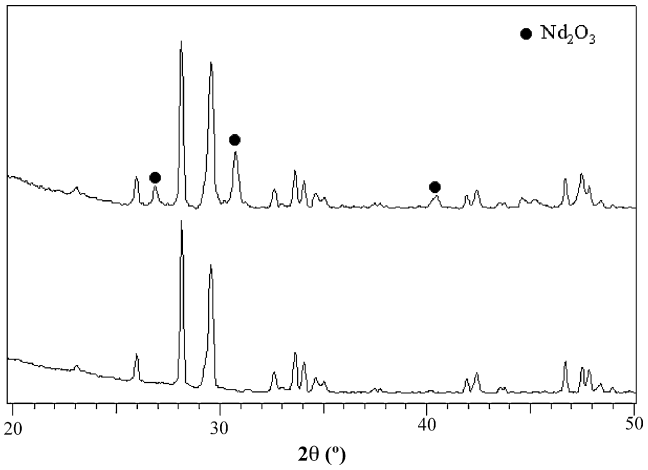

Fig. 6. XRD patterns of 10% Ni/$Nd_4Ga_2O_9$ catalyst (a) as prepared and (b) after TPR experiment.

No reduction peaks were observed for $Nd_4Ga_2O_9$, attesting to its stability as a catalyst support under hydrogen. However, three peaks labelled as α, β and γ were observed for the Ni/$Nd_4Ga_2O_9$ catalysts at 450–500 °C, 600 °C and 800–900 °C, respectively (Note that α peak overlaps β peak.).

The high temperatures of reduction indicate a strong and complex interaction between nickel and the cuspidine $Nd_4Ga_2O_9$ support. Therefore, since Ni^{2+} is not substituted for Ga^{3+} in $Nd_4Ga_2O_9$ (as mentioned above), this result suggests that besides NiO dispersed on the surface of $Nd_4Ga_2O_9$, several nickel phases such as Ga_2NiO_4 [10] and Nd_2NiO_4 [11] could have been formed during the synthesis of the catalysts. Few TPR data concerning the systems Nd–Ni–O and Ga–Ni–O have been reported in the literature, but by comparison with TPR profiles of La_2NiO_4 and $NiAl_2O_4$ [7–9], the analysis of the three reduction peaks observed in Fig. 5 can be done. The α peak can be assigned to the hydrogen uptake of surface NiO interacting weakly with the $Nd_4Ga_2O_9$ support. The β peak at 550–600 °C can be assigned to the reduction of Nd_2NiO_4 and the γ peak at 850 °C to the reduction of $NiGa_2O_4$. Since these phases were not detected by XRD they might exist on the surface of the $Nd_4Ga_2O_9$ crystals as thin layers not thick enough to be detected by XRD. However, after TPR experiences, extra peaks corresponding to Nd_2O_3 are observed in the XRD patterns of reduced catalysts (Fig. 6), probably as a consequence of the reduction of Nd_2NiO_4.

In order to better visualize the microstructure of the Ni/$Nd_4Ga_2O_9$ materials, a TEM study was performed. The fresh catalysts are made of agglomerates of fine grains (∼50 to ∼100 nm) overlapping (Fig. 7), that prevent from recording high resolution images of the surface structure of crystals. The Nd/Ga, Ga/Ni and Nd/Ni experimental ratios measured by EDX analysis with a broad focused beam on several agglomerates, are in good agreement with starting compositions. However, an excess of Ni was identified on some parts showing a darker contrast.

Nevertheless, after TPR reaction, the microstructure of the catalysts is strongly modified. In fact, many particles of nanometric size can be observed at the edge of agglomerates (Fig. 8).

The EDX analysis of these particles, performed with a nanoprobe electron beam, allows to identify two types of nanoparticles: Ni metal particles supported on Nd-rich zones of the agglomerates (mainly Nd_2O_3) (Fig. 9) and Ni–Ga–O particles with various Ga/Ni ratios (Fig. 10).

The characteristic EDX spectra of both types of particles and of one of the agglomerates can be compared in Fig. 11. Since $Nd_4Ga_2O_9$ cannot be reduced, as demonstrated by the TPR study, these nanoparticles probably result from the reduction of different Ni species at the surface.

Therefore, TEM results support the hypothesis that, besides NiO finely dispersed at the surface of Ni/$Nd_4Ga_2O_9$ fresh catalysts, Nd_2NiO_4 and Ga_2NiO_4 phases are also present. The complex microstructure observed in the reduced samples, confirms the strong interaction between Ni and the cuspidine $Nd_4Ga_2O_9$ support. This feature could prevent the tendency of

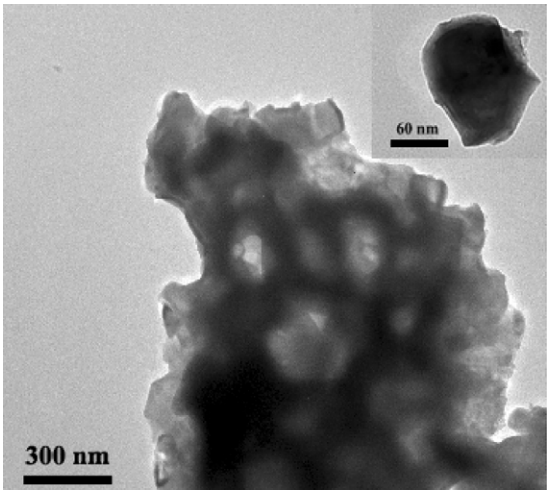

Fig. 7. TEM image of a typical agglomerate of fine grains observed in Ni/$Nd_4Ga_2O_9$ fresh catalysts. A nanoparticle is shown as an inset.

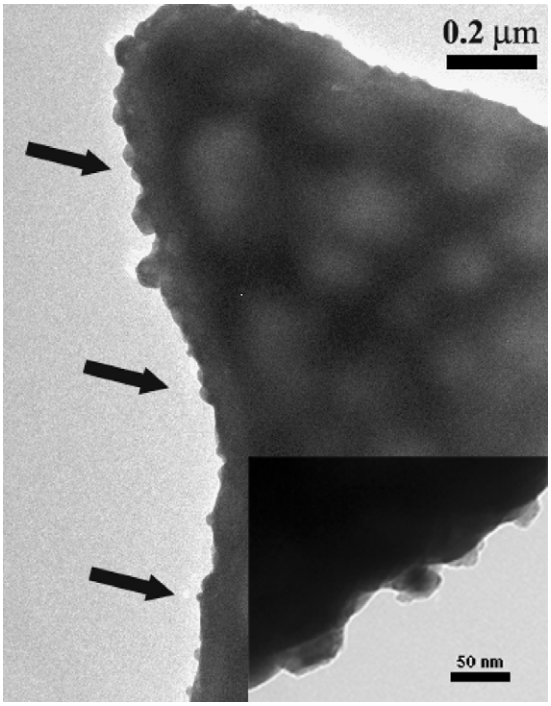

Fig. 8. TEM image showing the nanoparticles (see black arrows) observed at the edge of the agglomerates after TPR experience. An enlarged image of the edge is shown as an inset.

Ni to coarsening in the catalyst and increase the resistance to coking.

3.2. Catalytic dry reforming of methane

The activity of $Ni/Nd_4Ga_2O_9$ catalysts with different Ni contents was tested at 700 and 800 °C with an equimolar CH_4/CO_2 mixture. Since trace amounts of Nd_2NiO_4 were detected in the 15% $Ni/Nd_4Ga_2O_9$ catalyst, the evaluation was limited to 5% and 10% Ni catalysts.

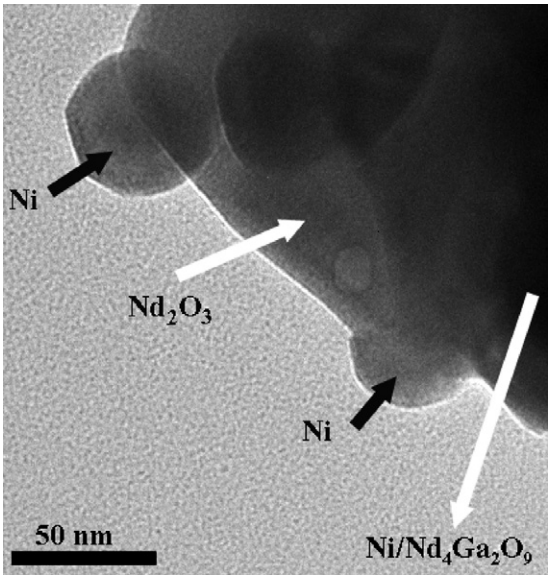

Fig. 9. TEM image of the Ni nanoparticles observed in the 10% $Ni/Nd_4Ga_2O_9$ catalyst after TPR.

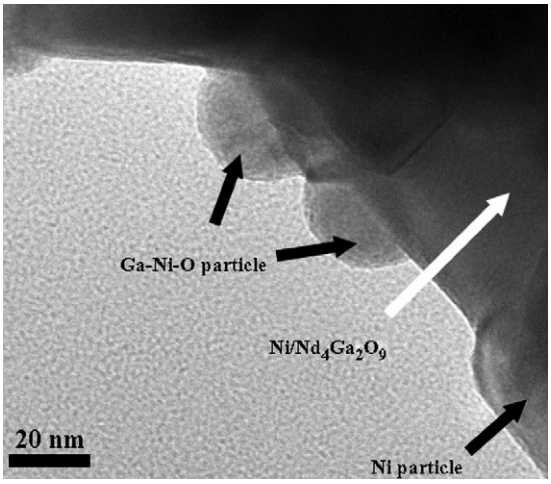

Fig. 10. TEM image of the Ga–Ni–O nanoparticles observed in the 10% $Ni/Nd_4Ga_2O_9$ catalyst after TPR.

The observed conversions of methane and carbon dioxide are listed in Table 2 showing that all catalysts exhibit an activity towards dry reforming of methane. The best was observed at 800 °C for the 10% Ni catalyst reduced at 700 °C. A plot of methane and CO_2 conversions as a function of time on stream over this catalyst at 800 °C is shown in Fig. 12. Initially, a slight deactivation was observed, but after ~2 h of reaction the catalytic activity remained nearly constant for 12 h. The increase of the reduction temperature led to a slight decrease of the activity at 800 °C, probably due to Ni coarsening in the catalyst. The nickel species resulting from the reduction, at temperatures higher than 700 °C, of Ni cations in minority phases at the surface (mainly $NiGa_2O_4$), seem to have a weak effect on the reaction. The carbon balance of the catalytic experiment and a subsequent thermogravimetric analysis (TGA) of the catalyst, under air, revealed that no carbon deposition occurred during the reaction.

A H_2/CO_2 molar ratio smaller than one and the lower conversion of methane compared to carbon dioxide strongly suggest that the reverse water gas shift reaction (RWGS) took place:

$$CO_2 + H_2 \rightarrow CO + H_2O$$

XRD patterns of the 10% $Ni/Nd_4Ga_2O_9$ spent catalysts (12 h on steam), reduced at 700 and 850 °C are displayed in Fig. 13 which shows that metallic Ni exists in both samples. The XRD pattern of the $Nd_4Ga_2O_9$ is also identified, demonstrating the stability of the support.

TEM micrographs of the 10% $Ni/Nd_4Ga_2O_9$ spent catalyst reduced at 700 °C, show (Fig. 14) that it is made of agglomerates of overlapping fine grains. The experimental contrast of the agglomerates is not homogeneous, as in the case of the fresh catalyst. Actually, zones exhibiting a brighter contrast coexist with dark zones, which present a Nd/Ga ratio in good agreement with that of the cuspidine phase. However a noticeable excess of Ni with respect to the starting composition

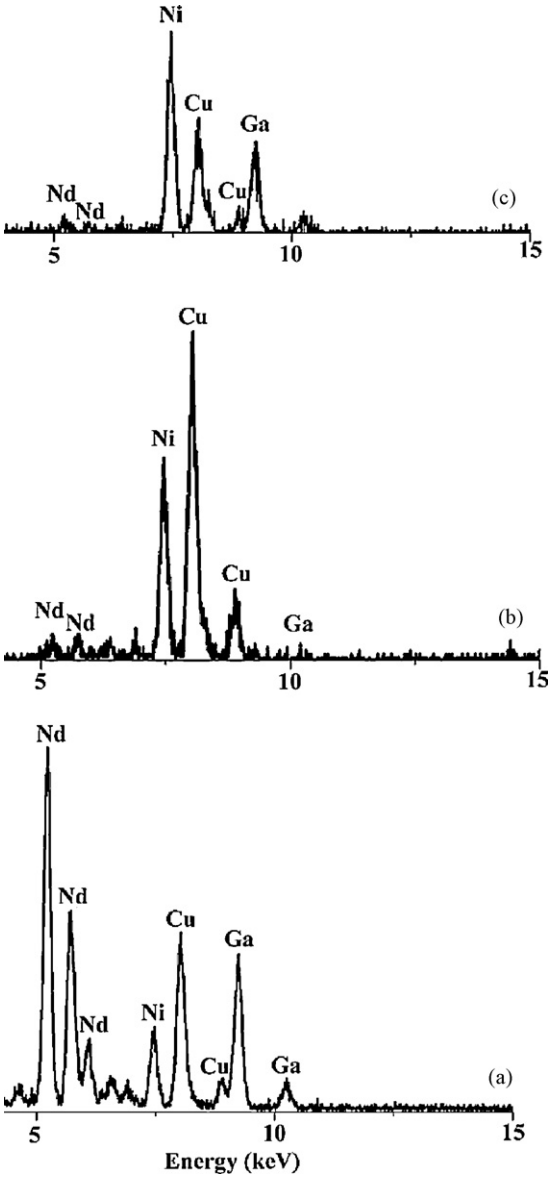

Fig. 11. Characteristic EDX pattern of: (a) inner part of agglomerates, (b) Ni particles supported on the Nd-rich zones of the agglomerates and (c) Ni–Ga–O particles. Note that the Cu peak comes from the copper grid used to support microcrystals.

Table 2
CH_4, CO_2 conversion and H_2/CO ratio, after 12 h of reaction at 700 and 800 °C over Ni/$Nd_4Ga_2O_9$ with different Ni content

Catalyst %Ni	T_{red} (°C)	Conversion[a] 700 °C		Conversion[b] 800 °C		F_d 800 °C	Ratio H_2/CO
		CH_4	CO_2	CH_4	CO_2		
5	700	12	25	14	31	0.7	0.3
10	700	48	65	69	82	0.89	0.8
10	850	20	30	60	76	0.97	0.6

Deactivation factor (F_d) = final conversion of CH_4/initial conversion of CH_4.
[a] 1.5 h on stream.
[b] 12.5 h on stream.

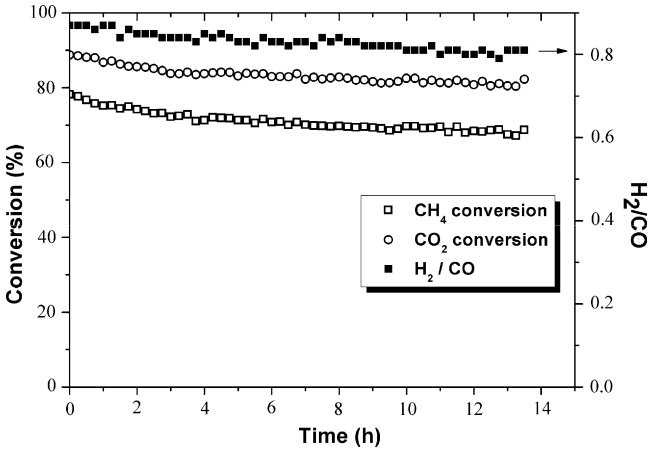

Fig. 12. Conversion of CO_2, CH_4 and molar ratio H_2/CO, observed over 10% Ni/$Nd_4Ga_2O_9$ catalyst reduced at 700 °C, as function of time on stream.

of the catalyst was found. The brighter zones are made up of $Nd_4Ga_2O_9$ nanocrystals supporting nearly spherical Ni particles of 10–20 nm in size. Little sintering occurs under reaction conditions. Furthermore, no carbonaceous deposits were observed by TEM analyses.

It could plausibly be argued that the absence of coking is closely related to catalyst structure. Chen and Ren [12] studied

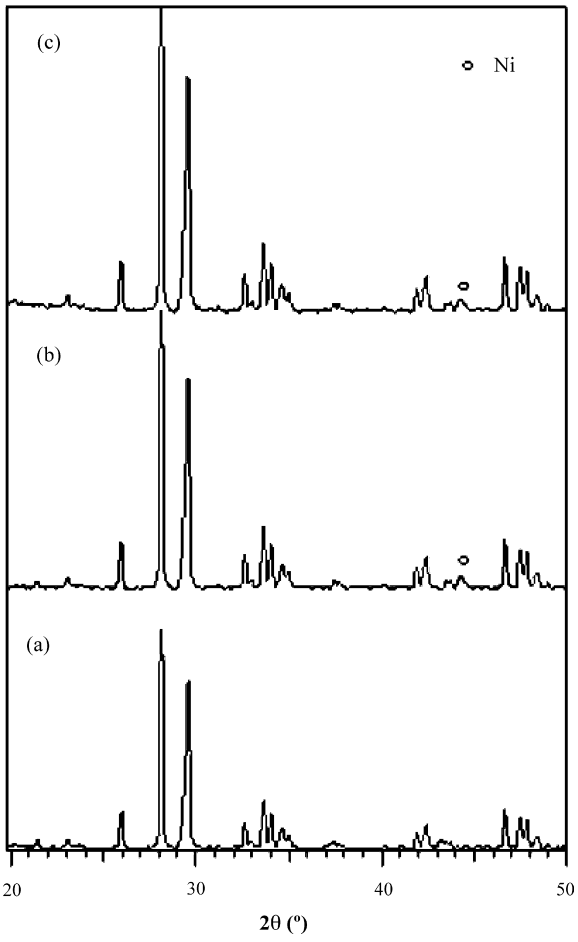

Fig. 13. XRD patterns corresponding to: (a) 10% Ni/$Nd_4Ga_2O_9$ fresh catalyst, (b) spent catalyst reduced at 700 °C and (c) spent catalyst reduced at 850 °C.

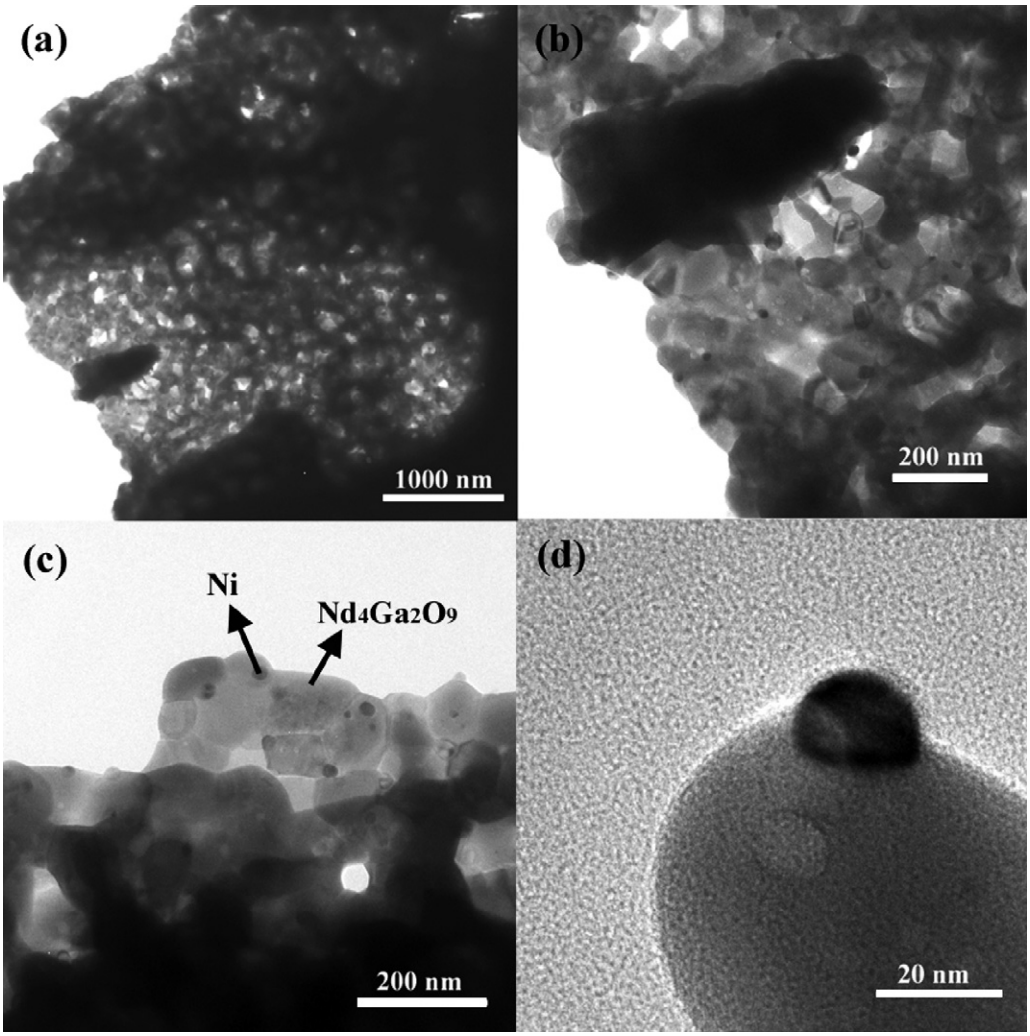

Fig. 14. TEM micrographs of the 10% $Ni/Nd_4Ga_2O_9$ spent catalyst reduced at 700 °C: (a) characteristic image of agglomerated grains, (b) and (c) enlarged images of a brighter contrast zone and (d) a typical Ni particle.

the CO_2 reforming of methane over Ni/Al_2O_3 and reported that the carbon deposition was markedly suppressed if spinel $NiAl_2O_4$ was formed during the synthesis of the catalysts. In our case, the $NiGa_2O_4$ phase formed at the surface could play a similar role. Furthermore, since the cuspidine-type support is an oxide of moderate basicity, the CO_2 chemisorption may promote the reaction with coke precursors and prevent coke accumulation.

Contrary to what was observed for the reduced catalyst at 950 °C (after TPR reaction), no Ni–Ga–O particles with $Ni/Ga \neq 1/2$ were observed in the 10% $Ni/Nd_4Ga_2O_9$ spent catalyst, reduced at 700 °C. This feature confirms that such particles result from the reduction of the $NiGa_2O_4$ surface phase, at temperatures >800 °C, as discussed before.

4. Conclusion

Carbon dioxide reforming of methane was studied over Ni catalysts supported on the cuspidine-like phase $Nd_4Ga_2O_9$. Attempts were made to prepare two types of materials by combustion synthesis: $Nd_4Ga_{2(1-x)}Ni_{2x}O_{9-x}$ compounds and $Ni/Nd_4Ga_2O_9$ samples containing 5, 10 and 15 wt% of Ni. The Ni-substituted $Nd_4Ga_2O_9$ phases could not be obtained whereas the $Ni/Nd_4Ga_2O_9$ catalysts were prepared successfully.

All catalysts exhibit activity towards dry reforming of methane. The best catalytic activity was observed at 800 °C, for the catalyst with a Ni content of 10%, reduced at 700 °C.

The high temperatures of reduction observed in the TPR study, indicate a strong and complex interaction between nickel and the cuspidine $Nd_4Ga_2O_9$ support. This feature could prevent the tendency to Ni coarsening in the catalyst and increase the resistance to coking. Thus, after reduction at 700 °C and reaction, Ni particles were 10–20 nm in size indicating that little sintering occurred under reaction conditions. Moreover, no carbonaceous deposits were observed after 12 h on steam.

Acknowledgements

The authors are grateful to COLCIENCIAS and PICS program: ''Valorisation of natural gas and Fischer-Tropsch synthesis'' for the financial support given.

V. Garcia Rojas and G. Sierra Gallego thank COLCIENCIAS and the University of Antioquia for their Ph.D. scholarship.

References

[1] O. Joubert, A. Magrez, A. Chesnaud, M.T. Caldes, V. Jayaraman, Y. Piffard, L. Brohan, Solid State Sci. 4 (2004) 1413–1418.
[2] A. Chesnaud, O. Joubert, M.T. Caldes, S. Ghosh, Y. Piffard, L. Brohan, Chem. Mater. 16 (2004) 5372–5379.
[3] C. Hwang, T. Wu, J. Wan, J. Tsai, Mater. Sci. Eng. B 111 (2004) 49–56.
[4] S.R. Jain, K.C. Adiga, V.R. Pai Verneker, Combust. Flame 40 (1981) 71.
[5] J. Schafer, W. Sigmund, S. Roy, F. Aldinger, J. Mater. Res. 12 (1997) 2518.
[6] T. Roisnel, J. Rodriguez-Carvajal, Physica B 192 (1993) 55.
[7] J. Guo, H. Lou, H. Zhao, D. Chai, X. Zheng, Appl. Catal. A: Gen. 273 (2004) 75–82.
[8] B.S. Liu, C.T. Au, Appl. Catal. A: Gen. 244 (2003) 181–195.
[9] J.M. Rynkowski, T. Paryjczak, M. Lenik, Appl. Catal. A: Gen. 126 (1995) 257.
[10] G. Li, L. Hu, J.M. Hill, Appl. Catal. A: Gen. (2006) 16–24.
[11] M. Lo Jacono, M. Schiavello, A. Cimino, J. Phys. Chem. 75 (1971) 1044.
[12] Y.G. Chen, J. Ren, Catal. Lett. 29 (1994) 39.